Generating multiple polarization outputs using random binary patterns with cascaded spatial light modulators

Ignacio Moreno,[a,b,*] Jeffrey A. Davis,[c] María del Mar Sánchez-López,[a,d] and Don M. Cottrell[c]
[a] Instituto de Bioingeniería, Universidad Miguel Hernández de Elche, 03202, Spain
[b] Departamento de Ciencia de Materiales, Óptica y Tecnología Electrónica, Universidad Miguel Hernández de Elche, 03202, Spain
[c] Department of Physics, San Diego State University, San Diego, CA 92182-1233, USA
[d] Departamento de Física Aplicada, Universidad Miguel Hernández de Elche, 03202, Spain

Abstract. In this work we apply an optical system with two cascaded liquid-crystal spatial light modulators (LC-SLMs) to produce multiple outputs with intensity and polarization control. We use a non-standard modulation configuration where the first LC-SLM operates as a phase-only modulator to encode a Fourier transform hologram multiplexing the desired multiple output beams, all with the same polarization. Next, the Fourier transform is optically formed onto the second LC-SLM, where each output beam is focused on different physical locations. The two SLMs have the LC director axis oriented horizontally. Thus, by rotating the linearly polarized output beams emerging from the first LC-SLM by 45º we operate the second LC-SLM as a variable retarder. Then, by applying different phase-shifts at the different areas of the second LC-SLM, we can vary the polarization state of each output beam. Finally, the output is imaged onto a camera detector to demonstrate the polarization states. Experimental results demonstrate the capability for this approach to encode a variety of output beams with different states of polarization.

Keywords: spatial light modulators, diffractive optical elements, multiplexing, polarization.

***Corresponding Author, E-mail: i.moreno@umh.es**

1 Introduction

Polarization beam splitters play a very relevant role in a number of applications and optical systems. Traditional polarizing beam splitters divide the beam in two orthogonal polarizations. However, recently there is an interest in dividing the beam into multiple beams. Polarization diffractive gratings (PDGs) create multiple beams with different states of polarization[1], with applications towards spectral and imaging polarimetry[2,3]. They can be fabricated with polarization sensitive holographic materials[4] and, more recently, by laser nanostructuring[5], with patterned liquid-crystals[6] or with metasurfaces[3].

Spatial light modulators (SLMs) can be as well used to display PDGs, having the great advantage of being reconfigurable at will controlled from a computer[7]. However, standard phase-only liquid-crystal (LC) SLMs only modulate the linear polarization component parallel to the LC director axis[8]. Therefore, PDGs are usually displayed on SLMs using systems where the beam passes twice through the device[9], or by using two SLMs[10], so two orthogonal polarization components can be independently phase-modulated. These previous approaches follow the traditional scheme used to generate vector beams[11,12], and requires a precise alignment between the two displayed phase gratings.

In this work we change this standard modulation scheme to generate PDGs, to a different configuration where the first LC-SLM is operated as a phase-only modulator to encode the inverse Fourier transforms of the desired multiple output beams, all with the same polarization, but with different physical locations. Next, the optical system forms the Fourier transform onto the second LC-SLM. By using a half wave plate to rotate the linear polarization by 45º, the second SLM is then used as a pixelated linear retarder where the retardance is spatially controlled with a displayed pattern. By applying different retardances in the regions where the output beams are focused, we can independently modify the state of polarization of each output. Therefore, the system results in a very effective way to generate PDG, with alleviated alignment restrictions compared to previous systems described above.

For the generation of the multiple outputs, we apply a random multiplexing approach[13] that we recently demonstrated useful in high resolution displays. This random technique allows the generation of independent output beams with arbitrary locations in the Fourier transform plane. In this work, we expand the approach to allow independent encoding of the polarization states of each output.

The paper is organized as follows. After this introduction, Section 2 introduces the experimental system. Then, Section 3 describes the random multiplexing technique and shows experimental results that demonstrate the generation of multiple beams with different states of polarization. Section 4 shows a different experimental demonstration of this approach where in addition each beam encodes a different spatial pattern. Finally, in Section 5, the conclusions of the work are presented.

2 Experimental System

Our experimental system is shown in Fig. 1. A He-Ne laser is spatially filtered and collimated with a converging lens (L1). The beam is polarized with a linear polarizer (P1). The system employs two parallel-aligned liquid-crystal on silicon (LCOS) SLM devices. These are reflective devices that are pixelated linear retarders where the retardance is controlled with the gray level of the image addressed from a computer[7]. When illuminated with linear polarization parallel to the LC director, they act as phase-only modulators[8]. On the contrary the linear polarization component perpendicular to the LC director is unaffected. We use two LCOS-SLMs from Hamamatsu, both of them model X10468-01, with 792×600 pixels and a pixel spacing of $\Delta = 20$ µm. In both devices the LC director is oriented horizontal in the laboratory framework.

The transmission axis of the input polarizer (P1) is selected horizontal, so LC-SLM1 operates as a phase only modulator, fully modulating the input beam, and not changing the state of polarization. A Fourier transform phase-only hologram is displayed on LC-SLM1. Then, a 2f optical Fourier transform system is formed with the lens L2: the distance from LC-SLM1 to the lens L2 is the lens focal length, and the LC-SLM2 is located the same distance behind the lens L2. This way, the optical system forms the exact Fourier transform of the input SLM onto the second SLM. Note that, although they introduce losses, we use two beam splitters (BS1 and BS2) to make the system compact and ensure normal incidence onto the SLMs.

LC-SLM2 is used to control the state of polarization by changing its retardance. Therefore, we need to rotate the horizontal polarization emerging from SLM1. For that purpose. we add a half wave plate (HWP) oriented at 22.5° so the polarization reaching SLM2 is now oriented at 45°.

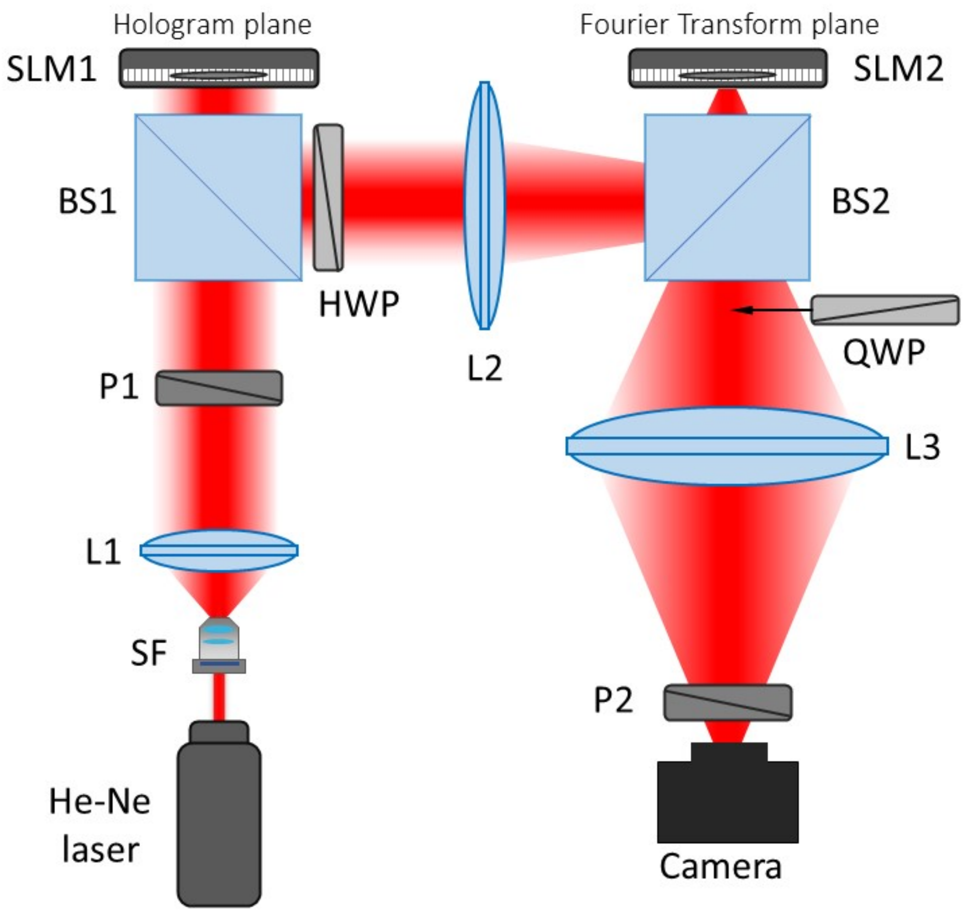

Fig. 1. Scheme of the optical setup. SF: spatial filter; L: convergent lens; P: linear polarizers; HWP: half-wave plate; QWP: quarter-wave plate; BS: beam splitter; LC-SLM: liquid-crystal spatial light modulator. The QWP is inserted when the output beams must be linearly polarized.

We show two possibilities for polarization control. In this above described situation, the retardance variations achieved at SLM2 by addressing different gray levels result in changes in the polarization state along the S2-S3 plane in the Poincaré sphere. For instance, when the SLM2 retardance is $\phi_2 = \pi/2$ or $\phi_2 = 3\pi/2$, the polarization reflected from SLM2 becomes right circularly polarized (RCP) or left circular circularly polarized (LCP) respectively. When the retardance is $\phi_2 = \pi$, then the reflected light is linearly polarized oriented at -45º. For intermediante values of ϕ_2 the reflected light is elliptically polarized with the ellipse azimuth always oriented at ±45º, but whose ellipticity changes with ϕ_2.

However, in many situations it is more interesting to produce polarization states that remain linear but where the orientation is controlled. We can achieve this case simply by adding a quarter-wave plate (QWP) oriented at 45º, located after SLM2 as indicated in Fig. 1. In this situation, the final beam is always linearly polarized, but the changes in the SLM2 retardance ϕ_2 result in changes on the orientation of the polarization[14].

Thus, the experimental system in Fig. 1 uses SLM1 to create a desired scalar complex distribution in the Fourier transform plane, i.e. with uniform polarization, and uses SLM2 to spatially modify the state of polarization to create the vectorial distribution. The final lens (L3 in Fig. 1) is used to image the SLM2 plane onto the camera detector sensor. In order to check the polarization properties of the light beam, a polarization analyzer (P2) is placed in front of the camera. A linear polarizer analyzer which is rotated is used to filter the linear components, and RCP and LCP analyzers are used to filter the circular components.

Next we describe the design of the phase mask addressed to the SLMs to achieve the desired control.

3. Phase Mask Designs and Experimental Results

In this approach, we consider P output beams, each one occupying a physically separated area of the output plane. As an example, we begin with $P = 4$ desired outputs, labeled as $f_m(x, y)$, $m = 1, \dots 4$, each one in a different quadrant in the output plane. The inverse Fourier transform of each output is calculated as $F_m(u, v) = \mathcal{F}^{-1}\{f_m(x, y)\}$. These Fourier transforms must be combined to yield a multiplexed phase-only hologram to be displayed on LC-SLM1.

For that purpose, we follow the random multiplexing approach[15,16], which has been shown to be very effective in modern high-resolution SLMs[13]. The multiplexing technique is quite simple. We begin with a random binary pattern where each pixel is assigned a value of 1 or 0. For convenience, we label this random binary pattern as $A(u, v)$. Next, we create the orthogonal pattern where we reverse the values in each pixel (pixels with value 1 in the original pattern are now assigned 0 value and vice-versa). We label this second pattern as $a(u, v)$. We now have two completely orthogonal patterns and can multiplex two different Fourier transforms by multiplying each by one of the two binary patterns.

We can increase the number of multiplexed patterns by forming a second independent binary random (1,0) pattern, which we label $B(u, v)$, and its corresponding orthogonal pattern $b(u, v)$. Now we can form four orthogonal patterns as $a_1 = AB$, $a_2 = Ab$, $a_3 = aB$, and $a_4 = ab$, where we omit the (u, v) dependence for simplicity. We have four binary amplitude patterns which fulfill the condition $a_m(u, v)a_n(u, v) = 0$ at all pixels when $m \neq n$.

Thus they can be used to multiplex four different Fourier transforms $F_m(u, v)$ by multiplying each by one of the four binary patterns, i.e., the multiplexed hologram $F(u, v)$ is given by:

$$F(u,v) = \sum_{m=1}^{P} a_m(u,v) F_m(u,v). \quad (1)$$

Considering SLM1 as an array of $N \times N$ pixels, each of the four patterns has a number of pixels given by $N^2/4$. Note that if $F_m(u,v)$ are all phase-only functions, the multiplexed hologram $F(u,v)$ is a phase-only function as well, and can be displayed directly in a phase-only SLM. Given the huge number of pixels available in current modern high-resolution SLMs[17], the random mask effectively generates the multiple beams. Next we show some experimental results.

3.1 Polarization beam splitter with four outputs

As a first example, we use $P = 4$ and divide the ouput plane into four quadrants of equal size. We can place any desired output into each quadrant as long as it does not extend beyond the quadrant. For this example, we place delta functions at the center of each quadrant. Figure 2(a) shows the four corresponding phase-only functions given from the inverse Fourier transform of each delta function. Here the phase levels from 0 to 2π are represented with gray levels. They are four blazed gratings diagonally oriented.

Next we multiply each of these full-sized blazed gratings by one of the binary masks mentioned earlier and the four patterns are added (Eq. (1)), resulting in the multiplexed mask shown in Fig. 2(b). The optical Fourier transform of each of the blazed gratings creates a single diffraction order, localized diagonally. Therefore, the multiplexed mask is expected to create the four orders simultaneously.

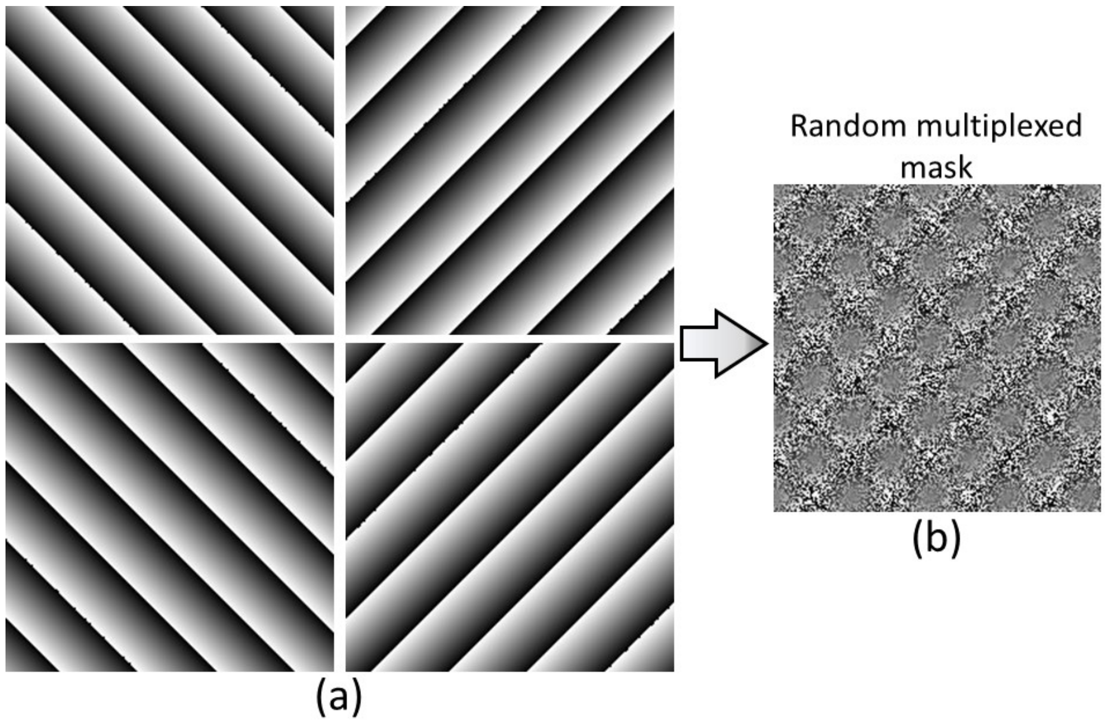

Fig. 2. Design of the phase mask in SLM1 to generated four ouputs. (a) expanded versions of the four linear blazed gratings made from the inverse Fourier transforms of the four delta funcitons, each located in the center of each of the four quadrants of the desired output plane. (b) Multiplexed mask using the random approach.

We first verified the effective generation of the four output beams in the Fourier plane. Figure 3 shows the experimental results. Figure 3(a) shows again the multiplexed phase mask displayed in SLM1 and Fig. 3(b) shows the corresponding experimental capture obtained at the camera detector. In this result no analyzer was placed before the camera. This image has been deliberately saturated to illustrate the successful effective generation of the four diffraction orders located at different positions on the SLM2 plane, with no significant impact of the random technique.

Next, we modify the state of polarization of the four beams by addressing different gray levels in the four quadrants of SLM2. Accordingly, a half wave plate is inserted after SLM1 to rotate the output orientation at 45º to the LC director axis of SLM2. We apply gray levels $g = 30$, $g = 85$, $g = 140$ and $g = 195$ in quadrants top left, top right, bottom right and bottom left respectively, which provide SLM2 retardances $\phi_2 = 2\pi$, $\phi_2 = 3\pi/2$, $\phi_2 = \pi$, $\phi_2 = \pi/2$, respectively. The expected polarization states are illustrated in Fig. 3(c). In this first experiment we do not place the QWP indicated in Fig. 1. Therefore, the expected polarizations of the output beams after being reflected at each quadrant of SLM2 are a diagonal linear state, a right circular state, an antidiagonal linear state and a left circular state, as shown in Fig. 3(c).

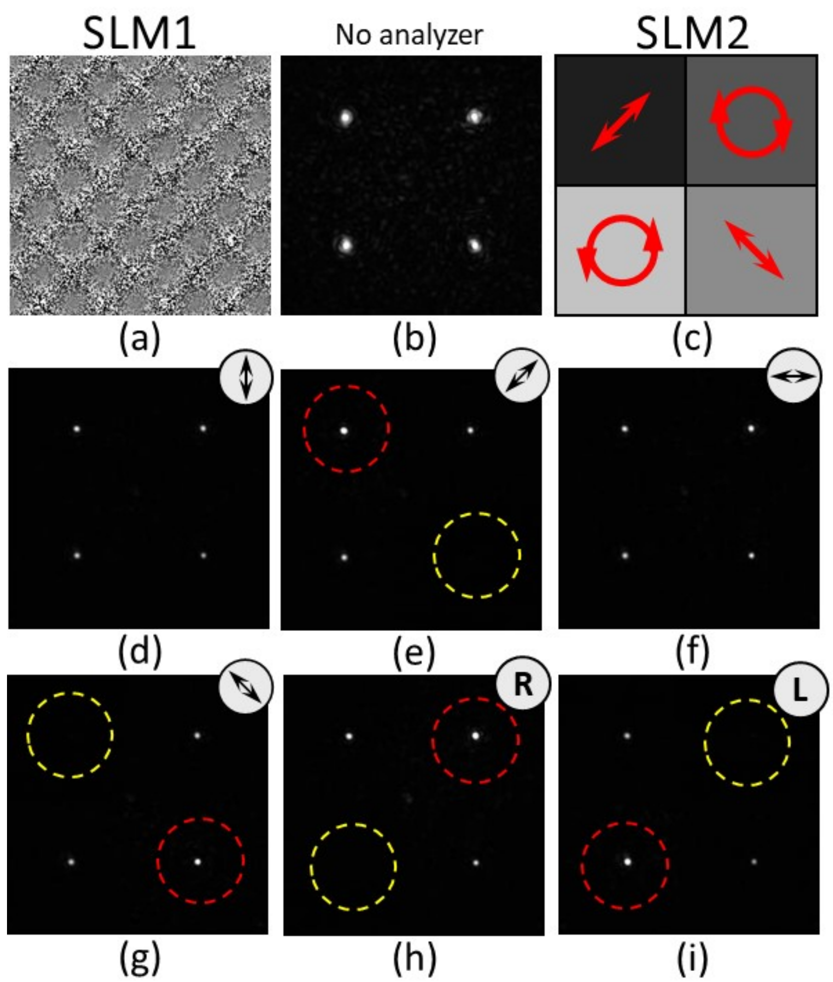

Fig. 3. (a) Multiplexed mask using the random approach with four outputs. (b) Experimental capture of the four diffraction orders without analyzer. (c) Four quadrant retardance pattern addressed to SLM2 and expected output polarizations. Experimental captures when an analyzer is placed in front of the camera: linear analyzer oriented (d) vertical, (e) diagonal, (f) horizontal and (g) antidiagonal, and circular analyzer (h) RCP and (i) LCP.

The polarization of each output beam is revealed by placing an analyzer in front of the camera. The images in Figs. 3(d) to 3(g) show the experimental capture when the analyzer is a linear polarizer oriented vertical (Fig. 3(d)), diagonal (Fig. 3(e)), horizontal (Fig. 3(f)) and antidiagonal (Fig. 3(g)), while Figs. 3(h) and 3(i) correspond to a RCP and a LCP analyzer. When the linear analyzer is oriented vertical or horizontal, the four output beams appear transmitted with the same intensity, as expected. On the contrary, when the linear analyzer is oriented diagonal or anti-diagonal, there is one output which is totally absorbed (indicated with a yellow circle) and another output beam which is fully transmitted (indicated with a red circle). This demonstrate that these outputs are linearly polarized along ±45º. The same situation happens to the other two output beams when we use the RCP and LCP analyzers, showing that these two outputs are circularly polarized with opposite helicity.

Figure 4 illustrates the polarization transformations in the system represented in the Poincaré sphere, a representation where the polarization transformations produced by the retarders can be easily visualized as rotations of the sphere[18]. Since the SLM2 LC director is oriented horizontal, the corresponding fast (F) and slow (S) eigenstates arethe horizontal and vertical linear polarization states. These states define the S1 axis of the Poincaré sphere. The polarization transformation induced by SLM2 can be visualized simply as a rotation of angle ϕ_2 around the S1 axis. Since the input state to SLM is the linear state with +45º orientation, this input state is represented at the positive S2 axis. Therefore, note that by changing the retardance ϕ_2 at SLM2 we could achieve any polarization state along the meridian in the S2-S3 plane of the Poincaré sphere, i.e. an elliptical state with arbitrary ellipticity but fixed orientation at ±45º (Fig. 4(a)). When the QWP is inserted after SLM2 in the system in Fig. 1, there is an additional polarization transformation. Since the QWP is oriented at 45º, now the visualization on the Poincaré sphere is another rotation now of

$\pi/2$ around the S2 axis. Therefore, all points lying in the green trajectory in Fig. 4(a) are now transformed by the QWP into a point lying in the equator of the Poincaré sphere (red curve in Fig. 4(b)). Therefore, the polarization of the output beams can be adjusted to any linear state with an arbitrary orientation controlled by the SLM2 retardance ϕ_2.

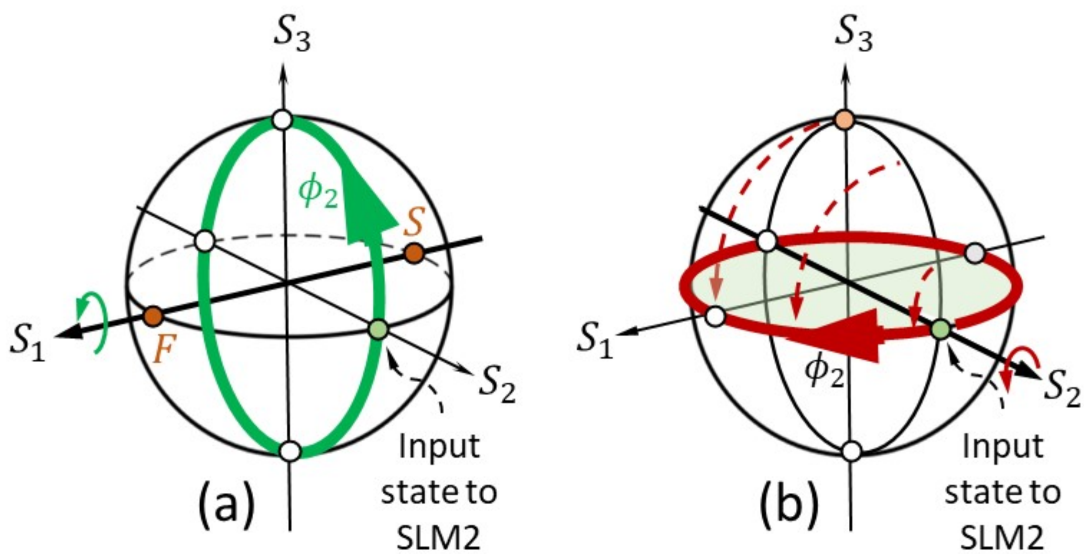

Fig. 4. Ilustration of the polarization transformations represented in the Poincaré sphere. (a) Transformation induced by SLM2. (b) Additional transformation induced by the QWP oriented at 45°.

The results in Fig. 5 correspond to this last situation where the QWP is inserted in the system. The gray levels addressed to SLM2 are the same as in Fig. 3, but now the insertion of the QWP in the system changes the polarization of the outputs in the top-right and bottom-left quadrants, which now become linearly polarized horizontally and vertically respectively. This is shown by the full extinction of one of these two outputs and the full transmission of the other when the linear analyzer is oriented horizontal or vertical (Figs. 5(d) and 5(f) respectively).

The other two beams in the other two quadrants have linear polarization oriented at ±45° and they are extinguished when the linear analyzer is oriented diagonal or antidiagonal respectively

(Figs. 5(e) and 5(g). For the two circular polarizer analyzers, the four beams appear transmitted with the same intensity, as expected from their linear polarization (Figs. 5(h) and 5(i)).

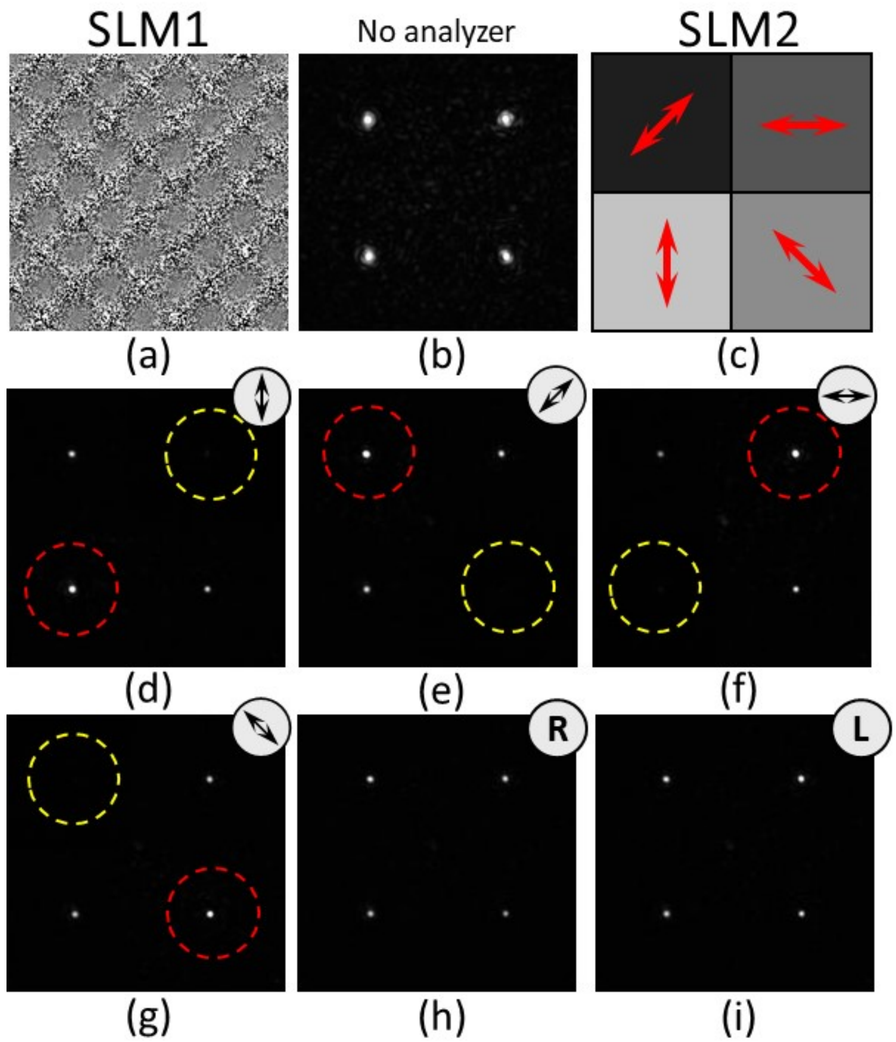

Fig. 5. (a) Multiplexed mask using the random approach with four outputs. (b) Experimental capture of the four diffraction orders without analyzer. (c) Four quadrant retardance pattern addressed to SLM2 and expected output polarization. The QWP is inserted in the system. Experimental captures when an analyzer is placed in front of the camera: linear polarizer analyzer oriented (d) vertical, (e) diagonal, (f) horizontal and (g) antidiagonal, and circular polarizer analyzer (h) RCP and (i) LCP.

3.2 Polarization beam splitterwith eight outputs

These previous results show the effective generation of a beam splitter with polarization control. Note that the diffraction orders generated by SLM1 can be positioned very easily on the four quadrants displayed by SLM2. Therefore, this procedure for creating PDGs offers a great advantage in terms of alignment compared to our previous approach[9] where we used two phase diffraction gratings encoded in two orthogonal polarizations.

To further illustrate this advantage, next we include a second example that shows results where we divide the input beam into $P = 8$ outputs. We divide the output plane into eight angular sectors and a delta function is placed at the center of each sector, forming a circular output pattern with an arrangement similar to a recently proposed vectorial diffractive element[19].

In order to multiplex the eight patterns, we need to create an additional random binary (1,0) pattern $C(u, v)$ and its orthogonal version $c(u, v)$. Now we can form eight orthogonal random patterns as the products $a_1 = ABC$, $a_2 = ABc$, $a_3 = AbC$, $a_4 = Abc$, $a_5 = aBC$, $a_6 = aBc$, $a_7 = abC$ and $a_8 = abc$. Thus, as before, we multiply each of the eight inverse Fourier transforms by one of these random binary patterns and use Eq. (1) to create the multiplexed hologram, now with $P = 8$.

Figure 6(a) shows the mutiplexed phase mask addressed to SLM1, which now includes eight linear phases oriented in diagonal, horizontal and vertical directions. Figure 6(b) shows the experimental capture when no analyzer is placed in front of the camera. This shows the effective generation of the eight equally intense output beams forming a circle of diffraction orders in the Fourier transform plane.

Now we assign a different retardance to each angular sector in the Fourier plane (SLM2) to create a radially linear polarization distribution. This requires the insertion of the QWP after SLM2 in the system. In order to accomplish the polarization transformation, SLM2 is addressed with a gray level mask like shown in Fig. 6(c), with gray levels $g = 30$, $g = 85$, $g = 140$ and $g = 195$, in a way that opposite slides have the same gray level. This crates the polarization states illustrated in Fig. 6(c).

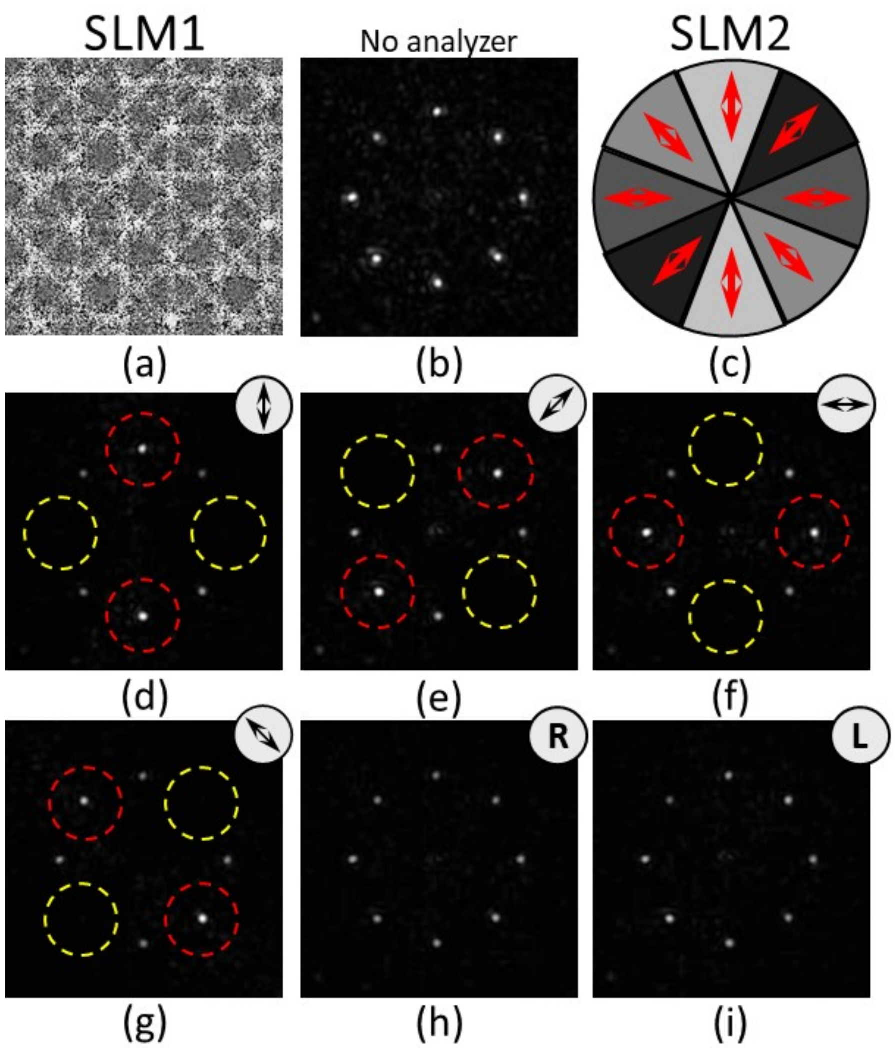

Fig. 6. (a) Multiplexed mask using the random approach with eight outputs. (b) Experimental capture of the eight diffraction orders without analyzer. (c) Retardance pattern addressed to SLM2 and expected output polarization. The QWP is inserted in the system. Experimental captures when an analyzer is placed in front of the camera: linear polarizer analyzer oriented (d) vertical, (e) diagonal, (f) horizontal and (g) antidiagonal, and circular polarizer analyzer (h) RCP and (i) LCP.

Figures 6(d) to 6(i) show the camera captures for the different analyzers placed in front of the camera. Again, we indicate with yellow and with red circles the diffraction orders wich are fully absorbed and fully transmitted by the analyzer. As expected, for each position of the linear analyzer, two orders are completely extinguished, and other two are fully transmitted. On the contrary, when the circular analyzers are used, the eight orders appear with the same intensity. These results therefore confirm the procedure.

4. Outputs with Arbitrary Shapes

Since these previous results are focused on the generation of PDGs, we only demonstrated output delta functions. In this Section we show how the same approach can be used for a general shaping of a light beam. As a final example, we consider a case where SLM displays the inverse Fourier transform phase-only hologram designed to create four outputs where now $\boldsymbol{f_n(x,y)}$ can have arbitrary shapes. We use a simple approach[20] to design a phase-only hologram, where each object image is multiplied by a binary (1,0) random pattern before calculating the inverse Fourier transform $\boldsymbol{F_n(u,v) = \mathcal{F}^{-1}\{f_n(x,y)\}}$. This way, when displaying this phase distribution on SLM1, the optical Fourier transform provides a reconstruction in the form of filled pattern[21], avoiding the classical edge enhanced effect that is produced in phase-only Fourier transform holograms[22].

Figure 7 shows the experimental results. Figure 7(a) shows the central part of the phase-only hologram, and Fig. 7(b) shows the capture in the Fourier plane, when there is no analyzer placed before the camera. This shows the effective generation of four different spatial patterns (a club, a heart, a spade and a diamond) with constant intensity, although affected by the speckle noise produced by the added random noise.

Next, we address SLM2 with a four sector pattern as scketched in Fig. 7(c), so each of the four spatial patterns have a different linear polarization. This is verified by placing the polarization analyzers in front of the camera. The captures shown in Figs. 7(d) to 7(g) confirm that each of the objects have a different linear polarization (horizontal, diagonal, vertical and anti-diagonal respectively). The results in Figs. 7(h) and 7(i) show the four objects with the same intensity, as expected when the analyzers are RCP or LCP filters.

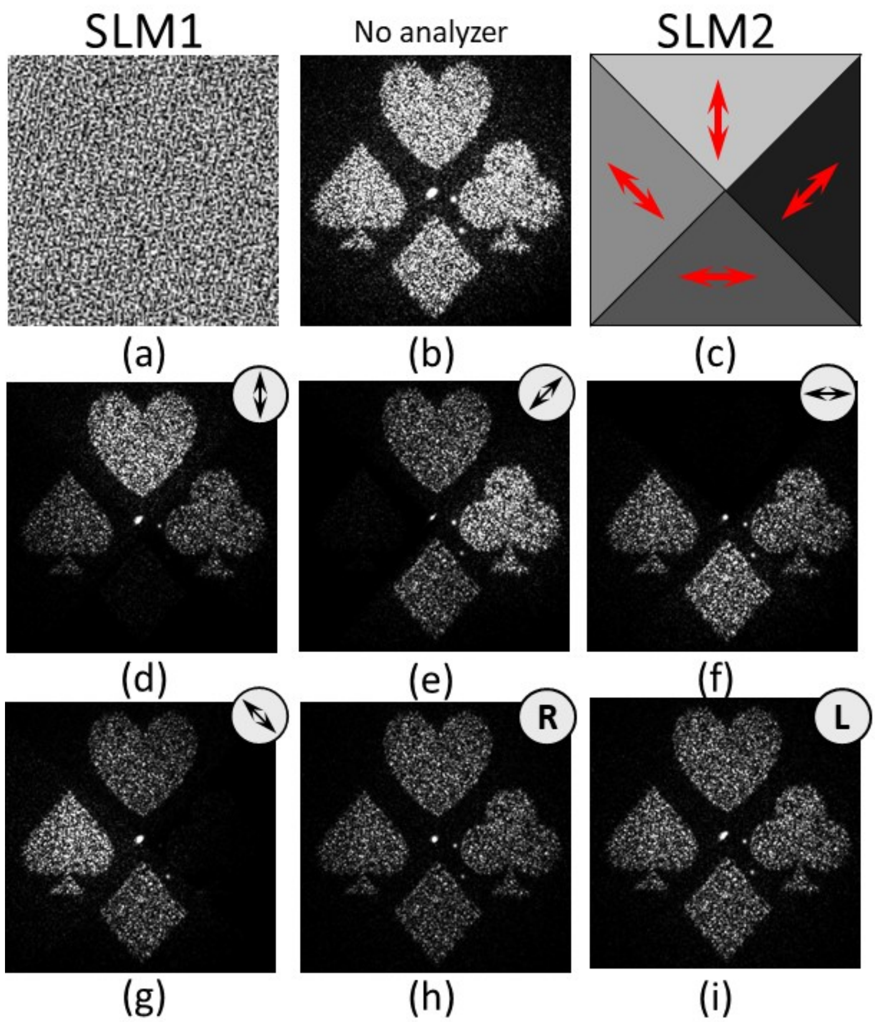

Fig. 7. (a) Phase-only computer-generated hologram designed to produce a circle of uniform intensity in the Fourier transform. (b) Experimental capture without analyzer. (c) Retardance pattern addressed to SLM2 and expected output polarization. The QWP is inserted in the system. Experimental captures when an analyzer is placed in front of the camera: linear polarizer analyzer oriented (d) vertical, (e) diagonal, (f) horizontal and (g) antidiagonal, and circular polarizer analyzer (h) RCP and (i) LCP.

5. Conclusions

In summary, we have demonstrated a simple technique to generate multiple output beams, each with a programmable polarization state. We use an optical system with two cascaded phase-only SLMs. But we modify the classical way of encoding, where each SLM encodes a phase function into two orthogonal polarizations states. In our approach, we use a first SLM to shape the intensity of the light beam with a phase-only hologram, thus not changing the polarization state, and we use a second SLM2 as a variable retarder to spatially modify the state of polarization. This alternative approach have advantages in terms of alignment, since the retardance sectors in SLM2 can be larger than the output patterns projected onto it. This is the case of the point objects (delta functions) as we employed in Figs. 3, 4 and 5, to create polarization diffraction grating patterns.

We show two kinds of polarization encoding. In the first case, we can program the ellipticity of the resulting output polarization states controlled through the retardance values of SLM2. Alternatively, we can change the orientation of the linearly polarized output beam simply by adding a QWP after SLM2. Experimental results have been presented where different polarization are shown for each case.

There are limitations to the approach. The method used to design the phase-only hologram displayed in SLM1 is a random multiplexing technique[13]. Thus, we are limited to the number of random binary patterns. As we increase the number of random binary patterns, the number of pixels available for each decreases. The technique might also be affected by fringing effects, which affect SLMs having a greater number of smaller pixels[13].

Secondly, we rely on the fact that the different output beams have different spatial locations projected onto the SLM2 screen. For simplicity we have generated delta function point objects. However each output can have a physical width, and this limits the number of retardance values that can be applied in SLM2. Nevertheless, the results in Fig. 7 have shown the polarization control of different wide shaped patterns. The polarization transformation has been illustrated with stepped functions addressed to SLM2 (shown in Figs. 3(c), 5(c), 6(c) and 7(c)). However it can be extended to produce produce continuous polarization variations onto an input beam shaped with SLM1. Thus, this represents an alternative way of producing vector beams, different to the classical way where two phase functions are encoded in two orthogonal polarizations.[11,12]

We expect that this approach can find different applications whenever multiple optical output beams with polarization control are required. Finally, let us also point out the capability of encoding amplitude and phase[23] onto all of these patterns.

Disclosures

The authors declare no conflicts of interest.

Data availability.

Data underlying the results presented in this paper are not publicly available at this time but may be obtained from the authors upon reasonable request.

Acknowledgements

IM and MMSL acknowledge financial support from Ministerio de Ciencia e Innovación, Spain (grant project PID2021-126509OB-C22) and Conselleria d'Innovació, Universitats, Ciència i Societat Digital, Generalitat Valenciana (grant project CIAICO/2021/276).

References

1. G. Cincotti, “Polarization gratings: design and applications”, *IEEE J. Quant. Electron.* **39**, 1645–1652 (2003). [https://doi.org/10.1109/JQE.2003.819526]
2. J. Kim and M. J. Escuti, “Demonstration of polarization grating imaging spectropolarimeter (PGIS)”, *Proc. SPIE* **7672**, 767208 (2010). [https://doi.org/10.1117/12.849758]
3. N. A. Rubin, P. Chevalier, M. Juhl, M. Tamagnone, R. Chipman and F. Capasso, “Imaging polarimetry through metasurface polarization gratings”, *Opt. Express* **30**(6), 9389-9412 (2022). [https://doi.org/10.1364/OE.450941]
4. L. Nikolova and P. S. Ramanujam, *Polarization Holography*, Cambridge University Press (2009).
5. M. Beresna and P. G. Kazansky, “Polarization diffraction grating produced by femtosecond laser nanostructuring in glass”, *Opt. Lett*. **35**(10), 1662-1664 (2010). [https://doi.org/10.1364/OL.35.001662]
6. R. Amano, P. Salamon, Y. Sasaki, S. Fujii, S. Yokokawa, F. Kobayashi, A. Buka, F. Araoka and H. Orihara, “Tunable two-dimensional polarization grating using a self-organized micropixelated liquid crystal structure”, *RSC Advances* **8**, 41472–41479 (2018). [https://doi.org/10.1039/C8RA08557A]
7. C. Rosales-Guzmán and A. Forbes, “How to shape light with spatial light modulators”, SPIE SpotLight (2017) [http://dx.doi.org/10.1117/3.2281295]
8. Z. Zhang, Z. You and D. Chu, “Fundamentals of phase-only liquid crystal on silicon (LCOS) devices”, *Light: Sci & Appl*. **3**, e213 (2014). [https://doi.org/10.1038/lsa.2014.94]
9. J. A. Davis, I. Moreno, M. M. Sánchez-López, K. Badham, J. Albero and D. M. Cottrell, “Diffraction gratings generating orders with selective states of polarization”, *Opt. Express* **24**(2), 907-917 (2016). [https://doi.org/10.1364/OE.24.000907]
10. A. Cofré, A. Vargas, F. A. Torres-Ruiz, J. Campos, A. Lizana, M. M. Sánchez-López and I. Moreno, “Quantitative performance of a polarization diffraction grating polarimeter encoded onto two liquid-

crystal-on-silicon displays", *Opt. Laser Technol.* **96**, 219–226 (2017). [https://doi.org/10.1016/j.optlastec.2017.05.027]

11. C. Maurer, A. Jesacher, S. Fürhapter, S. Bernet and M. Ritsch-Marte, "Tailoring of arbitrary optical vector beams", *New J. Phys*. **9**, 78 (2007). [https://doi.org/10.1088/1367-2630/9/3/078]
12. E. J. Galvez, S. Khadka, W. H. Schubert, and S. Nomoto, "Poincaré-beam patterns produced by nonseparable superpositions of Laguerre-Gauss and polarization modes of light", *Appl. Opt*. **51**(15), 2925-2934 (2012). [https://doi.org/10.1364/AO.51.002925]
13. J. A. Davis, I. Moreno, S. Gao, M. M. Sánchez-López and D. M. Cottrell, "Multiplexing onto a spatial light modulator using random binary pattern", *Opt. Eng.* **62**(10), 103104 (2023). [https://doi.org/10.1117/1.OE.62.10.103104]
14. J. A. Davis, D. E. McNamara, D. M. Cottrell and T. Sonehara, "Two-dimensional polarization encoding with a phase-only liquid-crystal spatial light modulator", *Appl. Opt.* **39**(10), 1549–1554 (2000). [https://doi.org/10.1364/AO.39.001549]
15. J. A. Davis, D. M. Cottrell, R. A. Lilly and S. W. Connelly, "Multiplexed phase-encoded lenses written on spatial light modulators", *Opt. Lett.* **14**(9), 420-422 (1989). [https://doi.org/10.1364/OL.14.000420]
16. J. A. Davis and D. M. Cottrell, "Random mask encoding of multiplexed phase-only and binary phase-only filters," *Opt. Lett*. **19**(7), 496-498 (1994). [https://doi.org/10.1364/OL.19.000496]
17. R. Li, Y. Ren, T. Liu, C. Wang, Z. Liu, J. Zhao, R. Sun and Z. Wang, "Generating large topological charge Laguerre–Gaussian beam based on 4K phase-only spatial light modulator", *Chinese Opt. Lett*. **20**(12), 120501 (2022). [https://opg.optica.org/col/abstract.cfm?URI=col-20-12-120501]
18. M. M. Sánchez-López1, P. García-Martínez, A. Martínez-García and I. Moreno, "Poincaré sphere analysis of a ferroelectric liquid crystal optical modulator: Application to optimize the contrast ratio", *J. Opt. A: Pure Appl. Opt*. **11**, 015507 (2009). [https://dx.doi.org/10.1088/1464-4258/11/1/015507]

19. A. Soria-Garcia, J. del Hoyo, L. M. Sanchez-Brea, V. Pastor-Villarubia, V. Gonzalez-Fernandez, M. Elshorbagy and J. Alda, “Vector diffractive optical element as a full-Stokes analyzer”, *Opt. Laser Technol*. **163**, 109400 (2023). [https://doi.org/10.1016/j.optlastec.2023.109400]
20. J. A. Davis, S. W. Flowers, D. M. Cottrell and R. A Lilly, “Smoothing of the edge-enhanced impulse response from binary phase-only filters using random binary patterns”, *Appl. Opt*. **28**(15), 2987–2988 (1989). [https://doi.org/10.1364/AO.28.002987]
21. I. Moreno, J. A. Davis, B. K. Gutierrez, M. M. Sánchez-López and D. M. Cottrell, “Multiple-order correlations and convolutions using a spatial light modulator with extended phase range”, *Opt. Laser Eng*. **146**, 106701 (2021). [https://doi.org/10.1016/j.optlaseng.2021.106701]
22. J. L. Horner and P. D. Gianino, “Phase-only matched filtering”, *Appl. Opt.* **23**(6):812–816 (1984). [https://doi.org/10.1364/AO.23.000812]
23. J. A. Davis, D. M. Cottrell, J. Campos, M. J. Yzuel and I. Moreno, “Encoding amplitude information onto phase-only filters”, *Appl. Opt*. **38**(23), 5004-5013 (1999). [https://doi.org/10.1364/AO.38.005004]

FIGURE CAPTIONS

Fig. 1. Scheme of the optical setup. SF: spatial filter; L: convergent lens; P: linear polarizers; HWP: half-wave plate; QWP: quarter-wave plate; BS: beam splitter; LC-SLM: liquid-crystal spatial light modulator. The QWP is inserted when the output beams must be linearly polarized.

Fig. 2. Design of the phase mask in SLM1 to generated four ouputs. (a) expanded versions of the four linear blazed gratings made from the inverse Fourier transforms of the four delta funcitons, each located in the center of each of the four quadrants of the desired output plane. (b) Multiplexed mask using the random approach.

Fig. 3. (a) Multiplexed mask using the random approach with four outputs. (b) Experimental capture of the four diffraction orders without analyzer. (c) Four quadrant retardance pattern addressed to SLM2 and expected output polarizations. Experimental captures when an analyzer is placed in front of the camera: linear analyzer oriented (d) vertical, (e) diagonal, (f) horizontal and (g) antidiagonal, and circular analyzer (h) RCP and (i) LCP.

Fig. 4. Ilustration of the polarization transformations represented in the Poincaré sphere. (a) Transformation induced by SLM2. (b) Additional transformation induced by the QWP oriented at 45°.

Fig. 5. (a) Multiplexed mask using the random approach with four outputs. (b) Experimental capture of the four diffraction orders without analyzer. (c) Four quadrant retardance pattern addressed to SLM2 and expected output polarization. The QWP is inserted in the system. Experimental captures when an analyzer is placed in front of the camera: linear polarizer analyzer oriented (d) vertical, (e) diagonal, (f) horizontal and (g) antidiagonal, and circular polarizer analyzer (h) RCP and (i) LCP.

Fig. 6. (a) Multiplexed mask using the random approach with eight outputs. (b) Experimental capture of the eight diffraction orders without analyzer. (c) Retardance pattern addressed to SLM2 and expected output polarization. The QWP is inserted in the system. Experimental captures when an analyzer is placed in front of the camera: linear polarizer analyzer oriented (d) vertical, (e) diagonal, (f) horizontal and (g) antidiagonal, and circular polarizer analyzer (h) RCP and (i) LCP.

Fig. 7. (a) Phase-only computer-generated hologram designed to produce a circle of uniform intensity in the Fourier transform. (b) Experimental capture without analyzer. (c) Retardance pattern addressed to SLM2 and expected output polarization. The QWP is inserted in the system. Experimental captures when an analyzer is placed in front of the camera: linear polarizer analyzer oriented (d) vertical, (e) diagonal, (f) horizontal and (g) antidiagonal, and circular polarizer analyzer (h) RCP and (i) LCP.

AUTHORS' BIOGRAPHY

Ignacio Moreno is professor of optics at University Miguel Hernández (UMH). He graduated in physics and received his PhD at Autonomous University of Barcelona (UAB). After two years at University of Valencia, he joined UMH. His research is centered in the field of spatial light modulators for diffractive and polarization optics. He is Fellow member of SPIE and Optica. In 2017-2020 he was President of the Spanish Optical Society (SEDOPTICA) and he is now Secretary of the European Optical Society (EOS).

Jeffrey A. Davis received his BS degree in physics from Rensselaer Polytechnic Institute and his PhD from Cornell University. He is a professor of physics at San Diego State University, where he leads the electro-optics program. His research interests include optical pattern recognition, spatial light modulators, and programmable diffractive optical elements. He is coauthor of more than 200 publications in peer-reviewed journals. He is a Fellow of SPIE and of Optica (former OSA).

María del Mar Sánchez-López is professor of applied physics at UMH. She graduated in physics and received her PhD at UAB. After a post-doc with INFM, Salerno (Italy), she joined UMH. Her research activity is centered on structured light and liquid-crystal devices. She is Senior member of SPIE. She is member of Real Sociedad Española de Física, where she served as President of its Local Section of Alicante (2017-2021).

Don M. Cottrell received his BS and PhD degrees from the University of Washington. He is an emeritus professor of physics at San Diego State University. His research interests include the computer construction of synthetic holograms and the computer program used in this research. He also conducts theoretical studies in general relativity and particle physics involving differential geometry and supersymmetry.